Phase transitions in $K_{1-x}Na_xNO_3$ embedded into molecular sieves

2009 J. Phys.: Condens. Matter 21 325902

(http://iopscience.iop.org/0953-8984/21/32/325902)

J. Phys.: Condens. Matter **21** (2009) 325902 (6pp) doi:10.1088/0953-8984/21/32/325902

Phase transitions in $K_{1-x}Na_xNO_3$ embedded into molecular sieves

S V Baryshnikov[1], E V Charnaya[2,3], A Yu Milinskiy[1], E V Stukova[1], Cheng Tien[3,4] and D Michel[5]

[1] Blagoveschensk State Pedagogical University, Blagoveschensk 675002, Russia
[2] Institute of Physics, St Petersburg State University, St Petersburg, Petrodvorets 198504, Russia
[3] Department of Physics, National Cheng Kung University, Tainan 70101, Taiwan, Republic of China
[4] Center for Micro/Nano Science of Technology, National Cheng Kung University, Tainan 70101, Taiwan, Republic of China
[5] Faculty of Physics and Geosciences, University of Leipzig, D-04103 Leipzig, Germany

Received 2 April 2009, in final form 3 July 2009
Published 23 July 2009
Online at stacks.iop.org/JPhysCM/21/325902

Abstract
Dielectric studies of molecular sieves MCM-41 filled with $K_{1-x}Na_xNO_3$ salts ($x = 0$, 0.05 and 0.10) were carried out and compared with results obtained for their bulk counterparts. The regular increase upon warming of the temperature of the reconstructive phase transition from phase II to phase I with decreasing pore sizes was observed for all x. A thermodynamic model for shifts of reconstructive phase transitions was suggested. Ferroelectric phase III was shown to occur upon cooling in bulk binary salts and for all x in confined geometry under the thermal conditions when phase III does not arise in bulk KNO_3. Ferroelectricity persisted below room temperature in the bulk binary salt with $x = 0.10$.

1. Introduction

A great deal of attention was recently focused on studies of nanostructured composites because of their importance for both fundamental and applied physics. Nanocomposites can be fabricated by filling porous matrices with various substances: metals, semiconductors, insulators, liquid crystals and others. Small particles confined within pores form an array whose geometry follows the geometry of the pore network. Filled porous matrices can bear different physical features depending on loaded substances. Late studies showed that properties of embedded particles are strongly affected by reduction of their sizes, interaction with pore walls and between particles (see, for instance, a review [1]). In particular, some confined substances had crystalline structures which did not coincide with that in bulk [2–4], superconductivity in porous matrices filled with metals was found to depend on strong and weak interparticle links [5] and melting–freezing transitions were shifted and diffused [6–8]. Confined geometry was also reported to influence remarkably the structural phase transitions including ferroelectric transitions. However, studies of ferroelectric nanocomposites are not numerous while those materials seem very promising, especially due to their potential applications in nonvolatile memory devices. The most investigated ferroelectrics within nanopores are sodium nitrite, mixtures with sodium nitrite, and Rochelle salt [9–13]. Other solid–solid phase transitions under confinement are even less studied (some results were reported in [14–17]). In the present paper we report results of dielectric studies of molecular sieves MCM-41 loaded with potassium nitrate, KNO_3, and KNO_3–$NaNO_3$ mixtures. The main goal of this work is to reveal the influence of confinement on structural phase transitions in $K_{1-x}Na_xNO_3$ with $x = 0$, 0.05 and 0.10, in particular, to demonstrate the possibility of the formation of the ferroelectric phase for small confined particles. Measurements on KNO_3 particles embedded into porous glasses with much coarser pores were reported in [18]. Properties of nanoporous matrices loaded with $K_{1-x}Na_xNO_3$ mixtures were not studied until now as far as we know.

2. Samples and experiment

Potassium nitrate (saltpeter), KNO_3, has long been used as an ingredient in explosives. The phase diagram for KNO_3 is cited in [19], for instance. At room temperature and pressure, KNO_3 crystallizes in an orthorhombic aragonite ($Pmcn$) phase. This phase is usually referred to as phase II. Upon heating to about 401 K it transforms to phase I, which has a disordered

rhombohedral $R\bar{3}m$ (calcite-type) structure. When phase I is cooled down from above 453 K at atmospheric pressure, the inverse transition I–II does not occur directly, but instead there is an intermediate phase III between about 397 and 383 K, which has the space group $R3m$. Transitions between phase II and phases I or III are reconstructive (they do not follow the group–subgroup relation). Phase III is ferroelectric. The occurrence of phase III depends on the thermal history of the sample and on pressure. At ambient pressure phase I transforms upon cooling directly to phase II when warmed not higher than about 450 K. The stability of phase III was found to improve for KNO_3 thin films [20] and particles confined within porous glasses [18] and on doping bulk KNO_3 with a small amount of sodium ions (see [21] and references therein).

Sodium nitrite, $NaNO_3$, crystallizes at room temperature in a rhombohedral ordered calcite $R\bar{3}c$ structure and transforms to a disordered calcite structure $R\bar{3}m$ upon warming [22].

The system $KNO_3/NaNO_3$ is one of the most studied binary salt systems, but the details of its phase diagram remains controversial. It was generally believed to be an example of continuous solid solutions: however, late studies attributed it definitely to eutectic systems (see [23] and reference therein). However, $K_{1-x}Na_xNO_3$ for $x \leqslant 0.1$ form substitutional solid solutions in phase I.

In the present studies, MCM-41 molecular sieves were used as nanoporous matrices. They have an ordered honeycomb structure of cylindrical pores with amorphous silica walls [24, 25]. The MCM-41 sieves were synthesized following [24, 25] with typical pore sizes of 37 and 26 Å as was found by electron microscopy and nitrogen adsorption–desorption isotherms. The calculated BET surface was 988 and 1150 $m^2\ g^{-1}$, respectively.

$K_{1-x}Na_xNO_3$ (pure potassium nitrate, KNO_3, and binary salts with $x = 0.05$ and 0.10) were embedded into mesoporous sieves from aqueous solution. The molecular sieve grains were put in such an amount of the salt-saturated solution that all the liquid penetrated into pores. The loaded sieves were dried and the procedure was repeated once more to promote better pore filling. Then the pellets were pressed under a pressure of about 7000 kg cm^{-2}. X-ray patterns of the pellets obtained showed only very weak narrow lines from bulk salts on the grain surfaces. The estimated amount of bulk salts was less than one-hundredth of the total amount used for the sample preparation and could not influence the experimental results. No reliable broadened peaks associated with confined small $K_{1-x}Na_xNO_3$ particles were observed.

Pellets of pressed $K_{1-x}Na_xNO_3$ powder counterparts were also prepared to compare the results of studies of bulk and confined materials. The binary salt powders were obtained by blending the KNO_3 and $NaNO_3$ water solutions of proper composition during 30 min and drying at 415 K.

The dielectric permittivity and conductivity were measured using an E7-12 immittance meter at a frequency of 1 MHz. The samples were warmed up from room temperature to 420 K and subsequently cooled back down. The temperature changes during the warming and cooling thermal cycles were not faster than 1 K min^{-1}. The temperature monitoring was better than 0.1°. The In–Ga eutectic was used as electrodes.

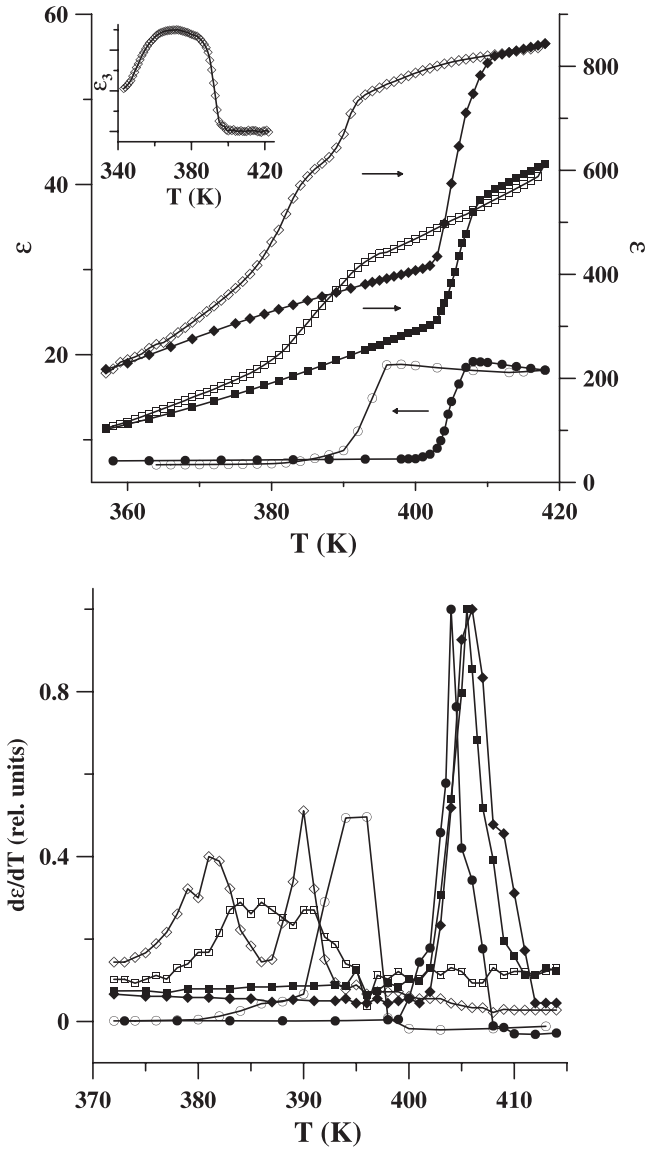

Figure 1. Dielectric permittivity ε (a) and first derivative $d\varepsilon/dT$ (b) versus temperature for bulk KNO_3 (circles) and KNO_3 loaded MCM-41 with pores of 37 Å (squares) and 26 Å (diamonds) obtained upon warming (closed symbols) and cooling (open symbols). Solid lines are guides for the eye. The inset to (a) shows the temperature dependence of the third-order nonlinear dielectric permittivity ε_3 upon cooling.

Before measurements the samples were dried at about 410 K to remove the adsorbed water.

3. Results

Temperature dependences of dielectric permittivity ε are shown in figure 1(a) for the bulk and confined KNO_3 samples. Dielectric anomalies correspond to structural phase transitions. Upon warming, the abrupt increase in permittivity of powdered potassium nitrate starts at 401 K, in good agreement with known data for the transition from phase II to phase I (see, for instance, [19, 26, 27]). For confined KNO_3 the similar steps in permittivity upon warming are shifted to high

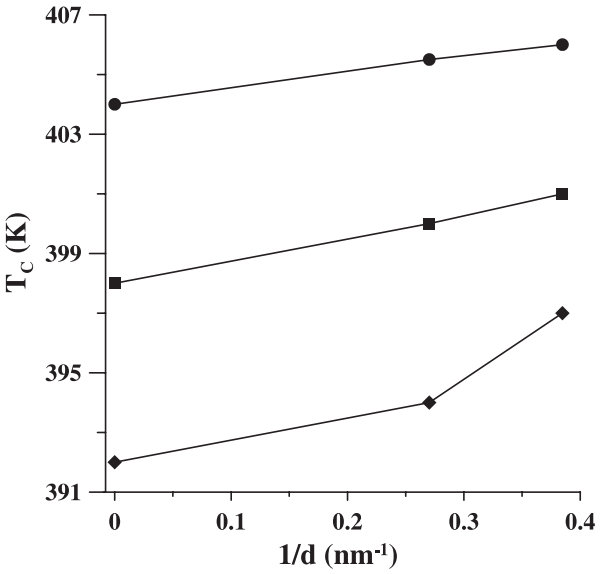

Figure 2. Temperature of the II–I phase transition T_c versus inverse pore size d for the $K_{1-x}Na_xNO_3$ salts with $x = 0$ (circles), 0.05 (squares) and 0.10 (diamonds). Solid lines are guides for the eye.

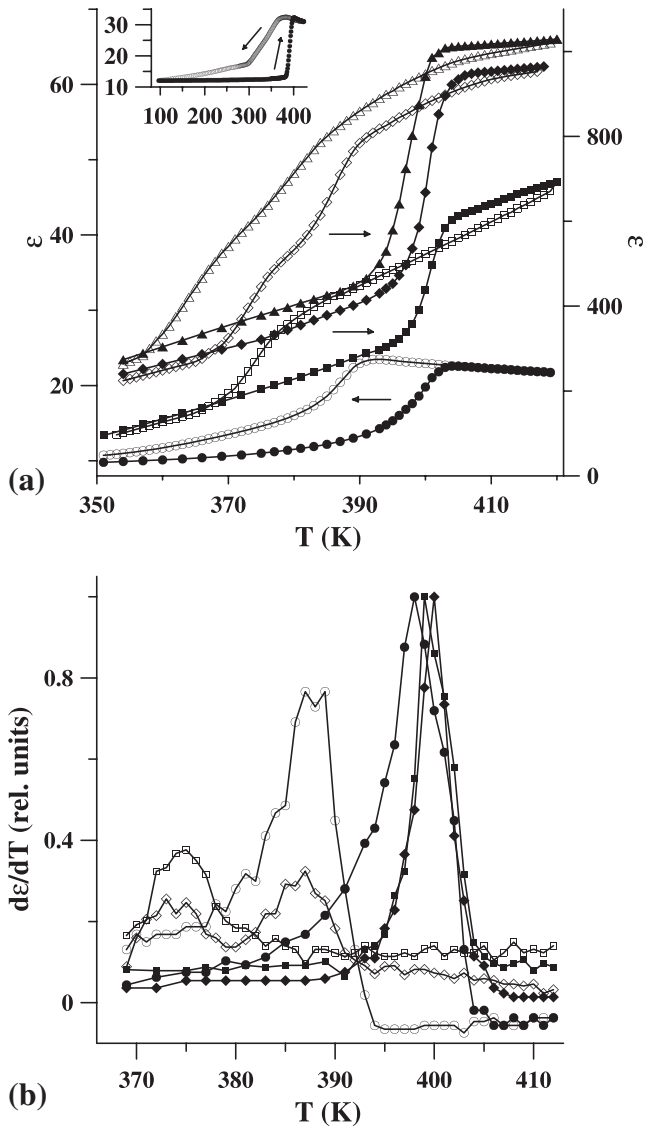

Figure 3. Dielectric permittivity ε (a) and first derivative $d\varepsilon/dT$ (b) versus temperature for bulk $K_{0.95}Na_{0.05}NO_3$ (circles), $K_{0.95}Na_{0.05}NO_3$-loaded MCM-41 with pores of 37 Å (squares) and 26 Å (diamonds) and dielectric permittivity (a) for $K_{0.9}Na_{0.1}NO_3$-loaded MCM-41 with pores of 26 Å (triangles) obtained upon warming (closed symbols) and cooling (open symbols). Solid lines are guides for the eye. The inset to (a) shows ε versus temperature for bulk $K_{0.90}Na_{0.10}NO_3$.

temperatures. Since the II–I transitions in all three samples are somewhat smeared, we define the phase transition temperature T_c as a point where the first derivative of permittivity with temperature, $d\varepsilon/dT$, is maximal (see figure 1(b)). The obtained values of T_c are listed in table 1. The dependence of T_c on pore size is also illustrated in figure 2. Note also the remarkable increase of the permittivity in confined potassium nitrate as compared with bulk (figure 1).

The transition temperatures observed upon warming and cooling for the bulk and confined KNO_3 samples are different, giving rise to a thermal hysteresis. For the powder potassium nitrate sample the onset of the permittivity decrease is near 396 K, which agrees with experimental data for the transition from phase I to phase II in bulk KNO_3 [19, 26, 27]. The hysteresis loop for this sample is quite symmetric (figure 1(a)), the temperature ranges of the phase transitions upon warming and cooling being very similar. This can also be seen in figure 1(b) from the $d\varepsilon/dT$ peak intensity and width upon warming and cooling.

When KNO_3 was embedded into pores of molecular sieves, the hysteresis loops become asymmetric and broadened (figure 1). While the onset of the phase transitions upon cooling is reduced only slightly, the permittivity curves obtained upon warming and cooling merge together at much lower temperatures. For the composite with pores of 26 Å a distinctive bend can be seen in the permittivity versus temperature curve upon cooling.

For bulk and confined binary salts the behavior of dielectric permittivity upon warming was rather similar to that observed for pure potassium nitrate, the shift of T_c varied depending on pore size and composition. However, for bulk binary salts the phase transition upon warming is more diffused than in bulk saltpeter. Some examples are shown in figure 3. The T_c values for binary salts obtained from permittivity measurements upon warming as maxima of $d\varepsilon/dT$ are listed in table 1. The temperature dependences of T_c on pore size at constant x are shown in figure 2. Note that, as for nanocomposites with pure potassium nitrate, porous matrices filled with binary salts show a pronounced enhancement of permittivity compared to their bulk counterparts (figure 3(a)).

The hysteresis loops observed during the warming–cooling runs in binary salts are strongly broadened even for pressed powder samples. For binary salts confined within 26 Å pores the permittivity curves taken on cooling show clear bends as for pure KNO_3. The phase transformation completion T_m associated with the temperature where the permittivity curves obtained upon cooling and warming merge together is strongly reduced, similar to the case of confined potassium nitrite.

Table 1. Temperatures T_c of the II–I phase transition upon warming and T_m of the phase transition completion upon cooling and difference ΔT between peaks of $d\varepsilon/dT$ upon warming and cooling for the samples under study.

	Pore size (Å)								
	Bulk			37			26		
x	T_c (K)	T_m (K)	ΔT (K)	T_c (K)	T_m (K)	ΔT (K)	T_c (K)	T_m (K)	ΔT (K)
0	404.0 ± 0.3	387 ± 1	9	405.5 ± 0.3	362 ± 1	22	406.0 ± 0.5	360 ± 1	25
0.05	398 ± 1	337 ± 3	11	400.0 ± 0.5	368 ± 2	25	401.0 ± 0.5	367 ± 2	28
0.10	392.0 ± 0.5	95 ± 5	54	394 ± 1	348 ± 2	36	397 ± 1	357 ± 2	30

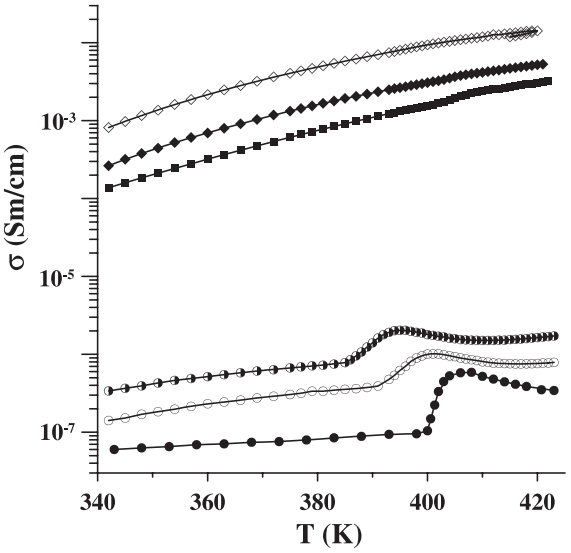

Figure 4. Temperature dependences of conductivity obtained upon warming. Closed, open and semiclosed circles correspond to bulk $K_{1-x}Na_xNO_3$ with $x = 0$, 0.05 and 0.10, respectively. Closed squares— KNO_3-loaded MCM-41 with pores of 37 Å. Closed and open diamonds—MCM-41 with pores of 26 Å filled with KNO_3 and $K_{0.9}Na_{0.1}NO_3$, respectively. Solid lines are guides for the eye.

The hysteresis width can be characterized by a difference ΔT between peaks of the $d\varepsilon/dT$ derivative upon warming and cooling. The ΔT values together with T_m found for all samples under study are collected in table 1. When two peaks of $d\varepsilon/dT$ were observed upon cooling, the top of the lower one was used to estimate ΔT.

The electric conductivity of pure powder potassium nitrate and nanocomposites with KNO_3 obtained upon warming is shown in figure 4. Confined geometry leads to an increase in conductivity by about four orders of magnitude. For powder binary salts and nanocomposites with binary salts, conductivity gradually increased with increasing x relative to the samples with pure KNO_3, as can be seen from examples depicted in figure 4. However, the influence of composition is much weaker than the effect of nanoconfinement. Both conductivity and permittivity demonstrated a continuous increase with decreasing frequency.

4. Discussion

The results obtained show pronounced alterations in the dielectric properties of powder and composite samples with decreasing particle size and increasing $NaNO_3$ amount.

Upon warming, the transition from the room temperature structure II to phase I is clearly seen for all samples under study. Confinement conditions provoke shifts of the II–I phase transition to high temperature for all x with respect to the bulk counterparts. The shifts grow regularly with decreasing pore sizes and increasing amounts of sodium nitrate (figure 2). The increase in T_c under confinement can be related to reduction of the sizes for particles formed within nanopores. Size effects on the solid–solid phase transitions were discussed for ferroelectric and antiferroelectric small particles within the framework of Landau theory and the Ising model (see [28–30] and references therein) and for superionic nanoparticles [31]. For phase transitions obeying the group–subgroup relation, the theoretical models predict a reduction of the phase transition temperature for ferroelectric particles in non-polar environments and an enhancement of the transition to the superionic state. In other words, the temperature range where the disordered phase occurs should generally narrow with decreasing particle sizes. However, the II–I phase transition belongs to the reconstructive type for which the models developed in [28–31] cannot be applied.

We suggest here a simple thermodynamic model of size effects on the reconstructive phase transition. Denote the Gibbs free energy of a small isolated particle in the low-temperature state by G_1 and that in the high-temperature state by G_2. Since the particle mass remains constant through the solid–solid phase transitions, the Gibbs free energies below and above the phase transition occurring at some temperature and pressure are equal to each other. For small particles the free energy should include the surface energy. Then G_1 at temperature T can be written as

$$G_1 = H_1 - TS_1 + \sigma_1 W_1, \tag{1}$$

where H_1 and S_1 are the enthalpy and entropy of the particle, σ_1 is the surface tension and W_1 is the particle surface. For a spherical particle $W_1 = 4\pi R_1^2$. G_2 is given by a similar relationship. At the phase transition temperature T_c $G_1 = G_2$ which yields

$$H_2 - H_1 - T_c(S_2 - S_1) + \sigma_2 W_2 - \sigma_1 W_1 = 0. \tag{2}$$

Taking into account that $S_2 - S_1 = (H_2 - H_1)/T_c^b$ (T_c^b is the phase transition temperature in bulk), $H_2 - H_1 = Lm$ (L is the specific latent heat of the phase transition and m is the particle mass) and $R_2/R_1 = (\rho_1/\rho_2)^{1/3}$ one can find for the shift of the spherical particle phase transition temperature $\Delta T = T_c^b - T_c$

the following relationship:

$$\frac{\Delta T}{T_c^b} = 3\frac{\sigma_1 - \sigma_2\left(\frac{\rho_1}{\rho_2}\right)^{2/3}}{L\rho_1 R_1}. \quad (3)$$

The obtained relation shows that the sign and value of the phase transition temperature shift depends on the surface tension below and above the phase transition and increases linearly with decreasing particle size. For confined particles the surface tensions can be modified by interaction with pore walls. Note that a relation similar to (3) can be obtained for the melting temperature shift in small spherical particles (see, for instance, [32, 33]). There are not enough data about surface tensions for binary KNO_3–$NaNO_3$ salts and pure potassium nitrate to compare the experimental results obtained in the present paper with equation (3). However, within the framework of the developed model one can conclude that the surface tension in phase I of pure potassium nitrate is smaller than that in phase II and that the difference between surface tensions in phases I and II increases with increasing x.

Among bulk samples the temperature T_c decreases with increasing x (figure 3 and table 1). This result agrees with known phase diagrams for the $K_{1-x}Na_xNO_3$ binary salts (see [23] and references therein). The trend toward the decrease in T_c with increasing admixture of sodium nitrate remains under confinement for samples with the same pore sizes, as can be seen in table 1.

Dielectric permittivity obtained for powder KNO_3 confirms that phase I directly transforms to phase II upon cooling as is known for bulk potassium nitrate when it was not warmed over 450 K [19]. This is not valid for the bulk binary salts and salts in confined geometry (figures 1 and 3). The broadened permittivity hysteresis loops characterized by ΔT with strongly diffused steps upon cooling and remarkably reduced temperatures T_m of the phase transitions completion show the occurrence of an intermediate crystalline structure. The general behavior of permittivity, especially the two resolved steps in nanocomposites with 26 Å pores and in bulk $K_{0.90}Na_{0.10}NO_3$, resembles the temperature dependences of permittivity observed in pure potassium sulfate after warming above 450 K [19]. The conformity of dielectric properties with the occurrence of ferroelectricity in pure and doped bulk saltpeter was confirmed previously (see, for instance, [18, 19]). Therefore, one can suggest that the ferroelectric phase III occurs upon cooling in all samples under study except pure potassium nitrate. To get an additional validation of the ferroelectric ordering we measured the third harmonic generation in a sinusoidal electric field for pure KNO_3 embedded in 37 Å pores since the third-order nonlinear constant ε_3 is known to increase through the ferroelectric phase transitions [34]. The result obtained is shown in the inset to figure 1(a). A remarkable increase in the third harmonic intensity was observed upon cooling while no noticeable anomaly was seen upon warming. Thus, the nanoscale confined geometry as well as the admixture of $NaNO_3$ facilitates the appearance of the ferroelectric crystalline modification. As can be seen from table 1, the admixture of $NaNO_3$ reduces T_m stronger than the decrease in salt particle sizes. For bulk $K_{0.90}Na_{0.10}NO_3$ the III–II phase transition was completed much below room temperature.

The results obtained in the present studies for $x = 0$ can be compared with those in [18] for pure potassium nitrate embedded in porous glasses with pore sizes of 23 and 160 nm. In [18] pure KNO_3 and porous glasses filled with KNO_3 were measured upon cooling down from 443 K. The intermediate ferroelectric phase was observed in all samples including pure potassium nitrate. For KNO_3 within pores of 23 nm in diameter the temperature range of phase III was found to be pronouncedly broadened. Contrary to [18], in the present paper the occurrence of ferroelectricity was observed for KNO_3 within molecular sieves under thermal conditions when phase III did not arise in bulk potassium nitrate.

The pronounced increase of conductivity and dielectric permittivity in nanocomposites relative to the bulk counterparts increases, likely due to space charge polarization which is often observed in nonhomogeneous materials (see, for instance, [35]). The necessary excess of mobile charges can be produced by structural imperfections on the confined particle surface.

In conclusion, dielectric studies of molecular sieves MCM-41 with pore sizes 37 and 26 Å filled with $K_{1-x}Na_xNO_3$ salts revealed the enhancement of temperatures of the reconstructive phase transition from phase II to phase I observed upon warming compared to their bulk counterparts. The shift of the phase transition temperatures increased with decreasing pore sizes. Such a shift can be understood within a thermodynamic model suggested for size effects on the reconstructive phase transition. Measurements of dielectric permittivity showed that the ferroelectric phase III occurs upon cooling in bulk binary salts and for all salts in confined geometry under the thermal conditions when this phase does not arise in bulk KNO_3. The phase transition completion temperatures upon cooling were found to decrease with increasing x for bulk and nanocomposite samples. Ferroelectricity persisted below room temperature in the bulk binary salt with $x = 0.10$. The pronounced increase in nanocomposite conductivity and permittivity relative to those in the bulk counterparts were treated as an effect of the space charge polarization.

References

[1] Kumzerov Yu A and Vakhrushev S B 2003 Nanostructures within porous materials *Encyclopedia of Nanoscience and Nanotechnology* ed H S Nalwa (California: American Science Publishers)
[2] Kilburn D, Sokol P E and Brown C M 2008 *Phys. Rev.* B **78** 214304
[3] Bellissent-Funel M-C, Lal J and Bosio L 1993 *J. Chem. Phys.* **98** 4246
[4] Charnaya E V, Tien C, Lin K J and Kumzerov Yu A 1998 *Phys. Rev.* B **58** 11089
[5] Charnaya E V, Tien C, Lin K J, Kumzerov Yu A and Wur C-S 1998 *Phys. Rev.* B **58** 467
[6] Xu Q, Sharp I D, Yuan C W, Yi D O, Liao C Y, Glaeser A M, Minor A M, Beeman J W, Ridgway M C, Kluth P, Ager J W III, Chrzan D C and Haller E E 2006 *Phys. Rev. Lett.* **97** 155701

[7] Charnaya E V, Tien C, Lee M K and Kumzerov Yu A 2007 *Phys. Rev.* B **75** 144101
[8] Christenson H K 2001 *J. Phys.: Condens. Matter* **13** R95
[9] Pan'kova S V, Poborchii V V and Solov'ev V G 1996 *J. Phys.: Condens. Matter* **8** L203
[10] Vakhrushev S B, Kumzerov Yu A, Fokin A, Naberezhnov A A, Zalar B, Lebar A and Blinc R 2004 *Phys. Rev.* B **70** 132102
[11] Tien C, Charnaya E V, Lee M K, Baryshnikov S V, Sun S Y, Michel D and Böhlmann W 2005 *Phys. Rev.* B **72** 104105
[12] Tien C, Charnaya E V, Lee M K, Baryshnikov S V, Michel D and Böhlmann W 2008 *J. Phys.: Condens. Matter* **20** 215205
[13] Vakhrushev S B, Golosovsky I V, Koroleva E Yu, Naberezhnov A A, Okuneva N M, Smirnov O P, Fokin A V, Tovar M and Glazman M 2008 *Phys. Solid State* **50** 1548–54
[14] Awschalom D D and Warnock J 1987 *Phys. Rev.* B **35** 6779
[15] Brown D W, Sokol P E and Ehrlich S N 1998 *Phys. Rev. Lett.* **81** 1019
[16] Mu R and Malhotra V M 1991 *Phys. Rev.* B **44** 4296
[17] Charnaya E V, Tien C, Lin K J and Kumzerov Yu A 1998 *J. Phys.: Condens. Matter* **10** 7273
[18] Poprawski R, Rysiakiewicz-Pasek E, Sieradzki A, Ciżman A and Polańska J 2007 *J. Non-Cryst. Solids* **353** 4457
[19] Chen A and Chernow A 1967 *Phys. Rev.* **154** 493
[20] Scott J F and Araujo C A 1989 *Science* **246** 1400
[21] Shimada S and Aoki T 1996 *Chem. Lett.* **25** 393
[22] Ghosh B P and Nag K 1984 *J. Therm. Anal.* **29** 433
[23] Berg R W and Kerridge D H 2004 *Dalton Trans.* **15** 2224
[24] Kresge C T, Leonowicz M E, Roth W J, Vartuli J C and Beck J S 1992 *Nature* **359** 710
[25] Jun S, Joo S H, Ryoo R, Kruk M, Jaroniec M, Liu Z, Ohsuma T and Terasaki O 2000 *J. Am. Chem. Soc.* **122** 10712
[26] Dessureault Y, Sangster J and Pelton A D 1990 *J. Chem. Phys.* **87** 407
[27] Zamali H and Jemal M J 1994 *Therm. Anal.* **41** 1091
[28] Zhong W L, Wang Y G, Zhang P L and Qu B D 1994 *Phys. Rev.* B **50** 698
[29] Jiang B and Bursill L A 1999 *Phys. Rev.* B **60** 9978
[30] Wang C L, Xin Y, Wang X S and Zhong W L 2000 *Phys. Rev.* B **62** 423
[31] Baryshnikov S V, Tien C, Charnaya E V, Lee M K, Michel D, Böhlmann W and Andriyanova N P 2008 *J. Phys.: Condens. Matter* **20** 025214
[32] Caupin F 2008 *Phys. Rev.* B **77** 184108
[33] Reiss H, Mirabel P and Whetten R L 1988 *J. Phys. Chem.* **92** 7241
[34] Ikeda S, Kominami H, Koyama K and Wada I 1987 *J. Appl. Phys.* **62** 3339
[35] Von Hippel A R 1995 *Dielectric Materials and Applications* (Boston, MA: Artech House Publishers)